Mechanochemically Synthesized Nanocrystalline Sb₂S₃ Particles

E. Dutková[a,*], M.J. Sayagués[b], C. Real[b], A. Zorkovská[a], P. Baláž[a], A. Šatka[c],
J. Kováč[c] and J. Ficeriová[a]

[a]Institute of Geotechnics, Slovak Academy of Sciences, Watsonova 45, 04001 Košice, Slovakia

[b]Institute of Material Sciences of Seville (CSIC-US), Spain

[c]Institute of Electronics and Photonics, Slovak University of Technology, Bratislava, Slovakia

Nanocrystalline Sb_2S_3 particles have been synthesized from Sb and S powders by high-energy milling in a planetary mill using argon protective atmosphere. X-ray diffraction, particle size analysis, scanning electron microscopy, energy dispersive X-ray spectroscopy, transmission electron microscopy, electron diffraction, high resolution transmission electron microscopy, UV-VIS, and differential scanning calorimetry methods for characterization of the prepared particles were applied. The powder X-ray diffraction pattern shows that Sb_2S_3 nanocrystals belong to the orthorhombic phase with calculated crystallite size of about 36 nm. The nanocrystalline Sb_2S_3 particles are constituted by randomly distributed crystalline nanodomains (20 nm) and then these particles are forming aggregates. The monomodal distribution of Sb_2S_3 particles with the average hydrodynamic parameter 210 nm was obtained. The quantification of energy dispersive X-ray spectroscopy analysis peaks give an atomic ratio of 2:3 for Sb:S. The optical band gap determined from the absorption spectrum is 4.9 eV, indicating a considerable blue shift relative to the bulk Sb_2S_3. Differential scanning calorimetry curves exhibit a broad exothermic peak between 200 and 300 °C, suggesting recovery processes. This interpretation is supported by X-ray diffraction measurements that indicate a 23-fold increase of the crystallite size to about 827 nm as a consequence of application of high temperature process. The controlled mechanochemical synthesis of Sb_2S_3 nanoparticles at ambient temperature and atmospheric pressure remains a great challenge.

1. Introduction

Antimony sulphide Sb_2S_3 is a kind of semiconductor material which has high photosensitivity and high thermoelectric power. Sb_2S_3 fulfils the optical requirements to obtain an electronic bandgap in the visible or the near-infrared (NIR) region, depending on its amorphous or crystalline nature [1]. The electronic gap of Sb_2S_3 lies around 2.2 eV (564 nm) for amorphous and 1.78 eV (697 nm) for crystalline Sb_2S_3 thin films [2]. Sb_2S_3 nanomaterials have been synthesized by different methods, such as solvothermal reaction, hydrothermal treatment, refluxing polyol process, sonochemical method, chemical vapor transport reaction, etc. [3–7].

The approach starting from solid state applies high-energy milling and is governed by mechanochemical methodology [8]. In this case, the solid reactions occur at the interfaces of the nanometer size grains that are continuously regenerated during milling. The high-energy milling has been used to synthesize various nanocrystalline chalcogenides [9–14]. We have already published a paper dealing with the synthesis and kinetics of mechanochemical synthesis of Sb_2S_3 and Bi_2S_3 nanoparticles obtained by high-energy milling [15]. In the present paper we concentrate our effort on the detailed structural and microstructural characterization of optimal Sb_2S_3 nanocrystalline sample synthesized by mechanochemical way from the point of view of the possible application of such material.

2. Experimental

2.1. Materials

Antimony powder (99.8%, Merck, Germany) and sulphur powder (99%, Ites, Slovakia) were supplied as reaction precursors.

Mechanochemical synthesis of Sb_2S_3 was carried out in a laboratory mill Pulverisette 6 (Fritsch, Germany) by high-energy milling. The following milling conditions were used — loading of the mill: 50 balls of 10 mm diameter; ball charge in the mill: 360 g; material of milling chamber and balls: tungsten carbide; weight of charge of the milled mixture of Sb and S precursors: 5 g, rotation speed of the planet carrier: 500 rpm; using a high purity argon atmosphere as a protective medium in the mill; milling time 60 min.

Sb_2S_3 particles have been synthesized in the mill according to the following reaction:

$$2Sb + 3S \rightarrow Sb_2S_3. \tag{1}$$

The reaction is thermodynamically possible, as the enthalpy change for reaction (1) is negative, $\Delta H^\circ_{298} = -169.4$ kJ mol^{-1} [16].

---

*corresponding author; e-mail: dutkova@saske.sk

2.2. Characterization methods

X-ray diffraction measurements were carried out using a D8 Advance diffractometer (Bruker, Germany) equipped with a θ/θ goniometer, Cu K_α radiation, secondary graphite monochromator and scintillation detector. Diffraction patterns were analysed with the Diffrac$^{\text{plus}}$ Eva analysis program for phase analysis and the Diffrac$^{\text{plus}}$ Topas program for the Rietveld analysis.

The particle size analysis was measured on Nanophox particle sizer (Sympatec, Germany) by the photon cross correlation spectroscopy method.

The microcharacterization of the samples was carried out using scanning and transmission electron microscopy (SEM and TEM). The following equipments have been applied: LEO 1550 field emission scanning electron microscope (Zeiss, Germany) and TECNAI G2 F30 STEM FEG, field emission scanning-transmission electron microscope, operating at 300 kV, coupled with an EDS INCA detector spectrometer.

Optical studies of the synthesized particles were carried out using UV-VIS spectrophotometer Helios Gamma (Thermo Electron Corporation, Great Britain).

The differential scanning calorimetric (DSC) diagram was monitored by a SETARAM scanning calorimeter DSC-11 with a sensitivity of 1 mV/s. All experiments were performed between 0 and 500 °C.

3. Results and discussion

The mechanochemical synthesis of Sb_2S_3 is illustrated by XRD patterns of the mixture of Sb+S precursors (a) and sample taken after 60 min of milling (b) (Fig. 1). In the starting material (pattern (a)) only peaks belonging to Sb metal (JCPDS 35-0732) and S (JCPDS 78-1888) are seen. The Sb_2S_3 (stibnite) crystallizes in the orthorhombic crystal structure (space group 62, P_{nma}). The refined lattice parameters are: $a = 11.3108$ Å, $b = 3.841$ Å, $c = 11.229$ Å. The diffraction peaks are broad due to grain refinement and lattice distortion of the material; only the peaks for Sb_2S_3 (JCPDS-70-9254) (pattern (b)) are shown, as no impurity phases are seen within this range. The kinetics of the mechanochemical synthesis was studied in paper [15]. Detailed analysis of XRD patterns has been performed. The estimated average crystallite size is $D = 36$ nm.

The particle size distribution of the nanocrystalline Sb_2S_3 particles is shown in Fig. 2. The nanosized dispersion has a monomodal distribution profile with average particle size of 210 nm.

The surface morphology of the mechanochemically prepared Sb_2S_3 particles characterized by SEM is depicted in Fig. 3. It shows that the product consists of small agglomerated particles with irregular morphology. During mechanochemical synthesis the particles are fractured and diminished.

The Sb_2S_3 sample obtained after 60 min of milling was analysed as well by ED, TEM, high resolution TEM (HRTEM) and energy dispersive X-ray spectroscopy
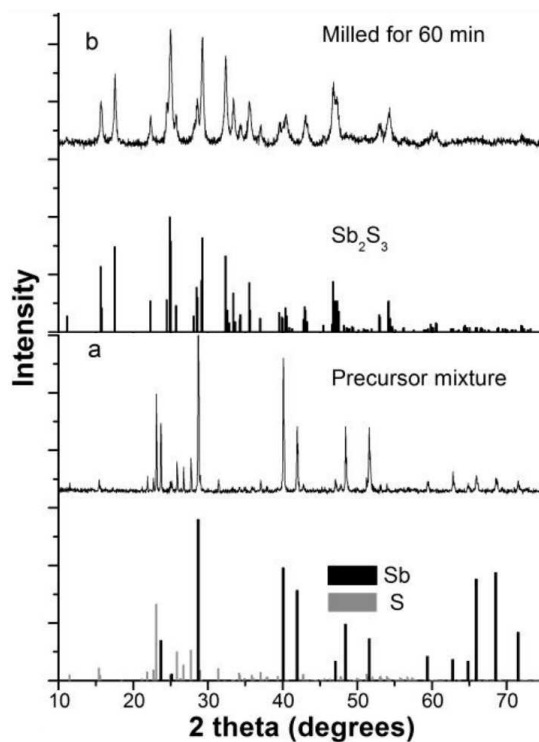

Fig. 1. XRD patterns documenting the mechanosynthesis of Sb_2S_3 particles. (a) Mixture of Sb and S precursors before milling, (b) synthesized sample after 60 min of milling.
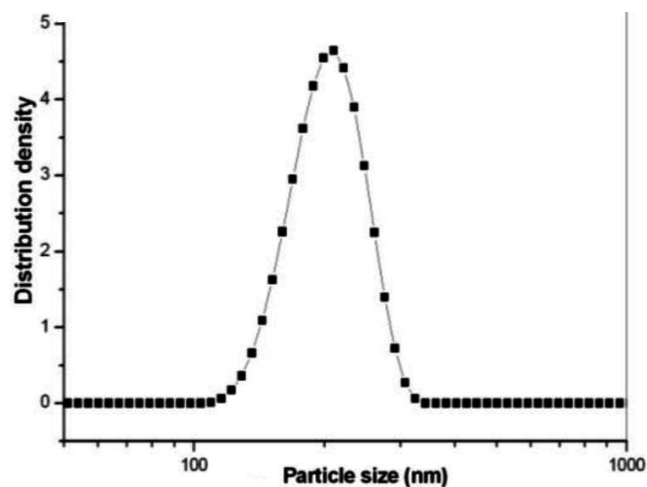

Fig. 2. Particle size distribution of Sb_2S_3 particles; milling time 60 min.

(EDS) techniques and the obtained results are depicted in Fig. 4. The powder sample is formed by agglomerated particles as can be seen in the TEM image (Fig. 4a). The corresponding ED (inset) is a ring pattern, indicating the small diffraction domain of the crystals; all the rings were indexed (the (*hkl*) planes are marked in the figure) in the orthorhombic system of the Sb_2S_3 sample with P_{nma} space group. The EDS spectrum (Fig. 4b) shows that the synthesized material is pure antimony sulphide with
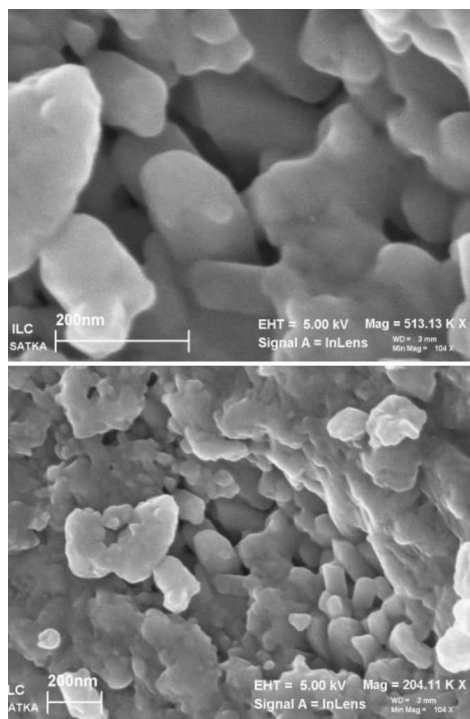
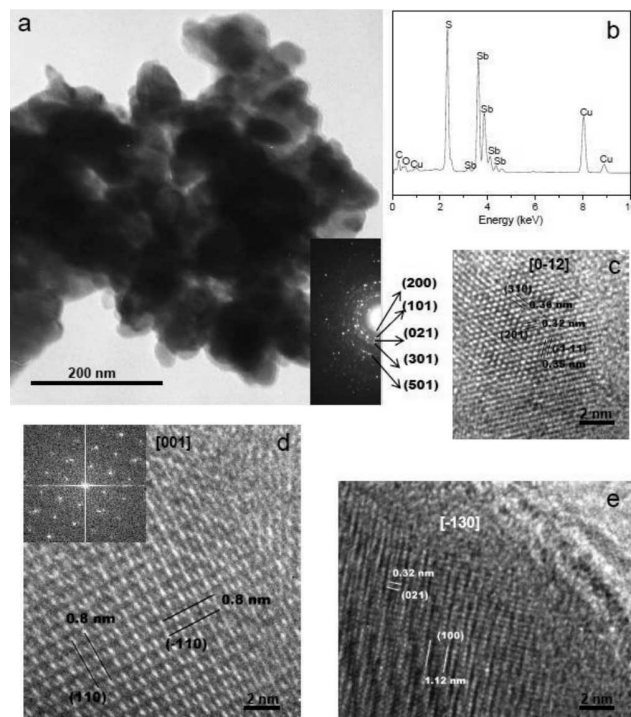Fig. 3. SEM image of Sb_2S_3 particles; milling time 60 min.

Fig. 4. Microstructure of the Sb_2S_3 sample obtained after 60 min of milling: (a) TEM micrograph and the corresponding ED-ring (inset), (b) EDS spectrum, (c–e) HRTEM micrographs.
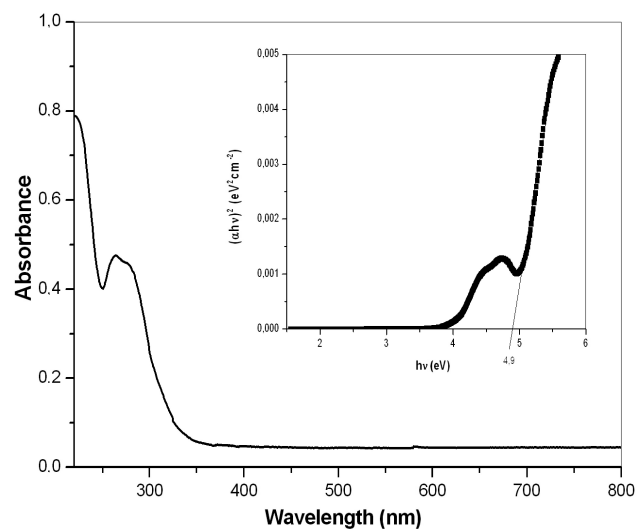
no detectable impurities; Cu and C peaks are coming from the grid. The elemental semiquantitative analysis indicates the Sb/S atomic ratio of 2/3 which is in good agreement with the formula. The HRTEM technique reveals that the particles are formed by small nanocrystals of different sizes. Only a few nanocrystals with really small size (about 5 nm) were found, one is presented in Fig. 4c. The presented nanocrystal is oriented along the [0–12] zone axis and the corresponding interplanar spacing is marked.

The majority of the nanocrystals were larger (about 20 nm) and two images are presented here. Figure 4d shows a crystalline nanodomain oriented along [001], the fast Fourier transform (FFT) in the inset reveals very good periodicity of the nanocrystals. Figure 4e presents a nanocrystal nearly oriented along [−130]. The interplanar spacing and (*hkl*) planes are also marked. The average crystalline nanodomain size found for Sb_2S_3 ($\approx$ 20 nm) is in good agreement with the XRD result and it is higher than for Bi_2S_3 (5–10 nm) [17] and particle size calculated with the photon cross correlation spectroscopy present similar tendency; about 210 nm for Sb_2S_3 and 198 nm for Bi_2S_3.

UV-VIS absorption spectrum of Sb_2S_3 nanoparticles (Fig. 5) shows absorption peak at about 270 nm. A bandgap of 4.9 eV was estimated by extrapolating the linear part of the Taue plot as shown in Fig. 5 (inset). An obvious blue shift was observed comparing with the bulk Sb_2S_3 at 721 nm (1.7 eV) due to quantum confinement. This is in a good accordance with literature [18].

Fig. 5. UV-VIS spectrum of the mechanochemically synthesized Sb_2S_3. Inset: the dependence of $(\alpha h\nu)^2$ versus $h\nu$.

Figure 6 shows the DSC curve obtained for the Sb_2S_3 mechanochemically synthesized for 60 min. The first run shows an endothermic peak at about 100 °C due to the loss of adsorbed water and a broad exothermic peak between 200–300 °C that can be related to the processes of recovery and re-crystallization of the defects generated during milling. The second and third run shows also a weak exothermic peak.
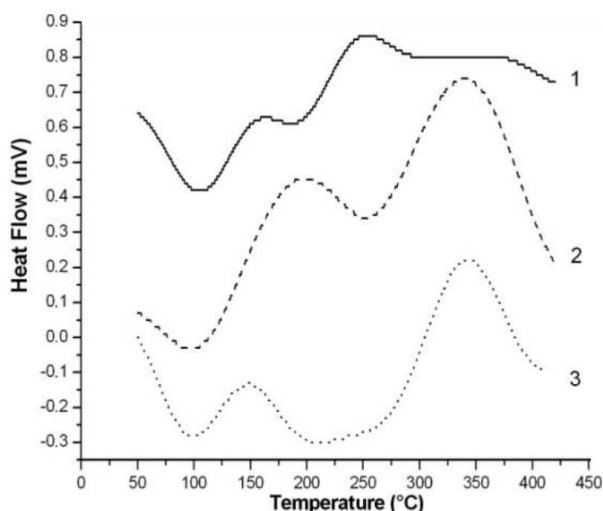
Fig. 6. DSC diagram of the mechanochemically synthesized Sb_2S_3 for 60 min. 1 — run1, 2 — run2, and 3 — run3.

Figure 7 shows the XRD patterns of the same sample before (Fig. 7A) and after (Fig. 7B) heating to $500\,°C$ during the DSC measurement. When this sample is heated in the calorimeter, the corresponding X-ray diagram shows the same peaks but quite narrow and well resolved. This is an evidence of good crystallinity, resulting from the processes indicated by the peak at $290\,°C$ in the DSC diagram. The estimated crystallite size after the three DSC cycles increased 23-fold to about 827 nm.
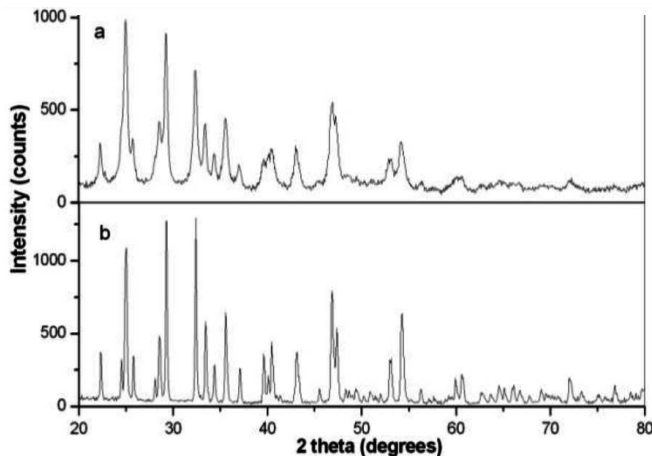

Fig. 7. XRD patterns of mechanochemically synthesized Sb_2S_3 for 60 min before DSC measurements (a) and after DSC measurements (b).

4. Conclusion

In summary, we have reported the preparation of the nanocrystalline Sb_2S_3 particles with average crystallite size 36 nm, using high-energy ball milling of elemental Sb-S powder mixtures in an argon atmosphere during 60 min. Heating to $500\,°C$ resulted in a 23-fold increase

of the crystallite size and in good thermal stability. Microscopic studies show that the particles are formed by agglomerated small nanocrystals with different sizes (5–20 nm). A blue shift was observed in the optical absorption edge of the synthetized nanomaterial. Although mechanochemical synthesis is a promising option for the preparation of Sb_2S_3 nanocrystalline particles, further investigations are needed to achieve control of the particle size and agglomeration.

References

[1] J. Li, M. Moskovits, T.L. Haslett, *Chem. Mater.* **10**, 1963 (1998).

[2] L.M. Ang, T.S.A. Hor, G.Q. Xu, C.H. Tung, S. Zhao, J.L.S. Wang, *Chem. Mater.* **11**, 2115 (1999).

[3] W. Quing-Sheng, Z. Guo-Xin, D. Ya-Ping, *J. Nanopart. Res.* **8**, 737 (2006).

[4] M.Y. Versavel, J.A. Haber, *Thin Solid Films* **515**, 7171 (2007).

[5] Q. Han, L. Chen, W. Zhu, M. Wang, X. Wang, X. Yang, L. Lu, *Mater. Lett.* **63**, 1030 (2009).

[6] K.-Q. Li, F.-Q. Huang, X.-P. Lin, *Scr. Mater.* **58**, 834 (2008).

[7] Y. Xu, Z. Ren, G. Cao, W. Ren, K. Deng, Y. Zhong, *Cryst. Res. Technol.* **44**, 851 (2009).

[8] P. Baláž, *Mechanochemistry in Nanoscience and Minerals Engineering*, Springer, Berlin 2008.

[9] E. Godočíková, P. Baláž, E. Gock, W.S. Choi, B.S. Kim, *Powder Technol.* **164**, 147 (2006).

[10] E. Godočíková, P. Baláž, J.M. Criado, C. Real, E. Gock, *Thermochim. Acta* **440**, 19 (2006).

[11] E. Dutková, P. Baláž, P. Pourghahramani, A.V. Nguyen, V. Šepelák, V. Feldhoff, J. Kováč, A. Šatka, *Solid State Ionics* **179**, 1242 (2008).

[12] P. Baláž, P. Pourghahramani, E. Dutková, M. Fabián, J. Kováč, A. Šatka, *Cent. Europ. J. Chem.* **7**, 215 (2009).

[13] E. Dutková, P. Baláž, P. Pourghahramani, S. Velumani, J.A. Ascencio, N.G. Kostova, *J. Nanosci. Nanotechnol.* **9**, 6600 (2009).

[14] P. Baláž, M. Achimovičová, M. Baláž, P. Billik, Z. Cherkezova-Zheleva, J. Criado, F. Delogu, E. Dutková, E. Gaffet, F.J. Gotor, R. Kumar, I. Mitov, T. Rojac, M. Senna, A. Streletskii, K. Wieczorek-Ciurowa, *Chem. Soc. Rev.* **42**, 7571 (2013).

[15] E. Dutková, L. Takacs, M.J. Sayagues, P. Baláž, J. Kováč, A. Šatka, *Chem. Eng. Sci.* **85**, 25 (2013).

[16] O. Kubaschewski, L.L. Evans, *Metallurgical Thermochemistry*, Pergamon Press, London 1955.

[17] E. Dutková, M.J. Sayagues, C. Real, P. Baláž, J. Kováč, A. Šatka, *Mater. Sci. Semicond. Proc.* **27**, 267 (2014).

[18] W. Qing Sheng, Z. Guo-Xin, D. Ya-Ping, *J. Nanopart. Res.* **8**, 737 (2006).